

## Density-functional theory of inhomogeneous systems of hard spherocylinders

E. Velasco

*Departamento de Física Teórica de la Materia Condensada, Universidad Autónoma de Madrid, Madrid E-28049, Spain*

L. Mederos

*Instituto de Ciencia de Materiales, CSIC, Cantoblanco, Madrid E-28049, Spain*

D. E. Sullivan

*Department of Physics and Guelph-Waterloo Physics Institute, University of Guelph, Guelph, Ontario, Canada N1G 2W1*

(Received 1 February 2000)

The smectic-A phase boundaries of a hard-spherocylinder fluid are calculated using a density-functional theory based on one proposed earlier by Somoza and Tarazona [Phys. Rev. A **41**, 965 (1990)]. Our calculations do not employ the translation-rotation decoupling approximation used in previous density-functional theories. The calculated phase boundaries agree well with computer simulation results up to aspect ratios  $L/D \approx 5$  and are in better agreement with the simulations than are previous theories. We generalize the model fluid by including long-range interactions with quadrupolar orientational symmetry, which are taken into account by mean-field approximation. For sufficiently large strength, these interactions produce a smectic-C phase, which undergoes either a continuous or weakly first-order transition to the smectic-A phase. The theory and numerical methods discussed here can be applied to the analysis of interfacial phenomena.

PACS number(s): 64.70.Md, 05.70.Fh

### I. INTRODUCTION

It was first shown by Onsager [1] that a fluid of hard spherocylinders could undergo a nematic ( $N$ )–isotropic ( $I$ ) phase transition. Onsager's analysis was based on a lowest-order (i.e., second-order) virial approximation to the free energy, which is accurate only in the limit of very long molecules. In recent years, computer-simulation studies have shown that hard spherocylinders of finite length exhibit an  $I$ – $N$  transition, as well as transitions to the layered smectic-A (SmA) phase [2,3]. The hard-spherocylinder model has also been studied using density-functional theory (DFT) [4–10]. Although based on approximations that generally yield results less accurate than those obtained from simulations, DFT has the advantage of being less time consuming, particularly in determining phase boundaries and for studying inhomogeneous systems.

However, as recently pointed out by van Roij *et al.* [8], previous DFT studies of smectic phases in hard-spherocylinder fluids have made the unphysical assumption that translational and orientational ordering are decoupled [5,6]. This approximation was dropped in a DFT analysis considered in Ref. [8], although the latter work was restricted to the low-density Onsager theory. One of the objectives of the present work is to remove the translation-orientation decoupling assumption of earlier DFT theories [5,6] and apply the resulting theory to hard spherocylinders of arbitrary density and elongation using a more accurate DFT approximation, which can also be used to study inhomogeneous systems with general spatial variations in order parameter and director orientation. We show that the coupling between orientational and translational degrees of freedom, which is certainly present, does not quantitatively affect the bulk phase behavior and that the theory reproduces well the *liquid* phase boundaries of this system obtained by Monte Carlo simula-

tions in Ref. [2]. However, the coupling is expected to be more relevant in other situations, such as wetting and anchoring phenomena at interfaces [11], where the present approximation can be used directly.

The practical relevance of a hard-core model to the study of real liquid crystals is based on the idea that repulsive intermolecular forces are mainly responsible for fluid structure, a notion deeply grounded in modern perturbation theories of fluids [12]. Implementation of perturbation theory for liquid crystals with more realistic intermolecular potentials requires an accurate assessment of the behavior of a suitable reference model such as the hard-spherocylinder fluid. This model has advantages with respect to other hard-core models of liquid crystals used in recent studies, such as hard ellipsoids, since the latter model does not exhibit a Sm-A phase [13].

A second objective of the present work is to test the suitability of the model as a reference system by including long-range intermolecular interactions with quadrupolar orientational symmetry, which are treated by a simple mean-field approximation. Several studies, beginning with work by Priest [14], have shown that interactions of this symmetry are able to induce formation of the smectic-C (Sm-C) phase, which is characterized by an average tilt of the molecular axes with respect to the smectic layer normal [15]. The same type of interaction has also been shown to account for tilted textures at free surfaces of nematic liquid crystals [16,17]. Recently, there have been several DFT studies of SmC phases based on models incorporating both hard-core and quadrupolar interactions, although these works have been limited either by restricting the molecules to be in perfect parallel alignment [18] or by using a hard-ellipsoid model for the repulsive cores [19]. The model used in Ref. [19] has the disadvantage that additional long-range interactions of appropriate orientational symmetry must be included to gener-

ate smectic ordering. In consequence, this model did not produce a  $N$ -Sm-A-Sm-C (NAC) point where the three orientationally ordered phases simultaneously coexist, and also generated phase boundaries (e.g., Sm-A-Sm-C) having a too strongly first-order character. The present model, which is closely akin to that of Ref. [18], removes most of these defects, although we do find that the Sm-A-Sm-C transition changes from continuous to first order with increasing molecular elongation. In contrast with Ref. [18], due to relaxing the constraint of perfect molecular alignment, we find that the  $N$ -Sm-A transition is first order, in agreement with the simulations of Ref. [2].

As mentioned before, the ultimate goal of our studies is to develop an accurate and numerically tractable DFT theory for realistic models of liquid crystals that can be applied to more complex situations, such as those due to the presence of interfaces and accompanying phenomena like wetting and anchoring. Although the present work is confined to the analysis of macroscopically uniform liquids, the smectic phases examined here exhibit spatial modulation and (in the case of Sm-C) tilt ordering, and therefore involve most of the same complexities occurring in the presence of interfaces. Here we extend and refine several techniques developed in previous work [19,20] to facilitate the numerical solution of the DFT, which will also be applicable to more general studies involving interfaces.

## II. THEORY FOR HARD SPHEROCYLINDERS

### A. Theoretical model

Let  $\rho(\mathbf{r}, \hat{\Omega})$  be the one-molecule density distribution, giving the mean local density of molecules at position  $\mathbf{r}$  and with orientation  $\hat{\Omega} \equiv (\theta, \phi)$  of their principal axes. Without loss of generality this distribution can be factorized as  $\rho(\mathbf{r}, \hat{\Omega}) = \rho(\mathbf{r})f(\mathbf{r}, \hat{\Omega})$ , where  $\rho(\mathbf{r})$  is the number density distribution and  $f(\mathbf{r}, \hat{\Omega})$  accounts for the distribution of orientations. The decoupling of translational and orientational degrees of freedom at this level (which we will *not* assume) amounts to considering a spatially uniform  $f(\mathbf{r}, \hat{\Omega}) = f(\hat{\Omega})$ . For phases with orientational order this function is peaked around some direction  $\hat{\mathbf{n}}$ , called the director.

In density-functional theory one writes a free-energy functional of the one-molecule density distribution,  $F[\rho]$ , which can be split into ideal  $F_{\text{id}}[\rho]$  and excess  $F_{\text{ex}}[\rho]$  parts,  $F[\rho] = F_{\text{id}}[\rho] + F_{\text{ex}}[\rho]$ , where

$$F_{\text{id}}[\rho] = kT \int \int d\mathbf{r} d\hat{\Omega} \rho(\mathbf{r}, \hat{\Omega}) \{ \ln[\Lambda^3 \rho(\mathbf{r}, \hat{\Omega})] - 1 \} \quad (1)$$

with  $\Lambda$  the thermal wavelength,  $k$  Boltzmann's constant, and  $T$  the temperature. The excess part, which contains the effect of interactions, must be approximated for lack of an exact expression. A popular approximation, first introduced for spatially uniform phases [for which  $\rho(\mathbf{r}, \hat{\Omega}) = \rho f(\hat{\Omega})$ ,  $\rho$  being the mean number density] is the *decoupling approximation* (DA) [4,21,22]. The idea behind the DA is to map the free energy in terms of an effective system of hard spheres (HS's) of diameter  $\sigma$ :

$$\begin{aligned} \frac{F_{\text{ex}}[\rho]}{N} &= \frac{\Psi_{\text{ex}}^{\text{HS}}(\rho_{\text{HS}})}{V_{\text{exc}}^{\text{HS}}} \int d\hat{\Omega} \int d\hat{\Omega}' f(\hat{\Omega}) f(\hat{\Omega}') \\ &\times \int d\mathbf{r} V_{\text{exc}}(\mathbf{r}, \hat{\Omega}, \hat{\Omega}'), \end{aligned} \quad (2)$$

where  $V_{\text{exc}}^{\text{HS}}$  is the excluded volume of two spheres (equal to  $4\pi\sigma^3/3$ ),  $V_{\text{exc}}(\mathbf{r}, \hat{\Omega}, \hat{\Omega}')$  is the (orientation-dependent) excluded volume function of two hard spherocylinders

$$V_{\text{exc}}(\mathbf{r}, \hat{\Omega}, \hat{\Omega}') = \begin{cases} 1 & \text{if } \mathbf{r} \text{ is within the excluded volume} \\ 0 & \text{otherwise,} \end{cases} \quad (3)$$

and  $\Psi_{\text{ex}}^{\text{HS}}(\rho)$  is the excess free energy per molecule of a system of hard spheres. The effective density  $\rho_{\text{HS}}$  is usually chosen such that the packing fractions of the effective hard-sphere system and the real hard spherocylinders are the same. This condition alone is sufficient since the free energy of hard spheres is a function only of the packing fraction, i.e., of the product  $\rho_{\text{HS}}\sigma^3$ , but not of  $\rho_{\text{HS}}$  or  $\sigma^3$  separately. The DA is equivalent to a scaling of all virial coefficients of order higher than 2 in terms of those of a system of hard spheres [23].

Since our aim in this paper is the study of highly nonuniform liquid-crystalline systems (bulk smectic phases being a particular case), a proper non-local density-functional approximation must be used. One may envisage several ways to generalize the DA in order to make it nonlocal [18]. Following Somoza and Tarazona (ST) [5], we use the generalized decoupling approximation

$$\begin{aligned} F_{\text{ex}}[\rho] &= \int d\mathbf{r} \frac{\Psi_{\text{ex}}^{\text{PHE}}(\bar{\rho}(\mathbf{r}))}{\bar{\rho}_{\text{PHE}}(\mathbf{r})} \int d\hat{\Omega} \rho(\mathbf{r}, \hat{\Omega}) \\ &\times \int \int d\mathbf{r}' d\hat{\Omega}' \rho(\mathbf{r}', \hat{\Omega}') V_{\text{exc}}(\mathbf{r} - \mathbf{r}', \hat{\Omega}, \hat{\Omega}'). \end{aligned} \quad (4)$$

Here  $\Psi_{\text{ex}}^{\text{PHE}}(\rho)$  is the (known) excess free energy of an effective system of parallel hard ellipsoids,  $\bar{\rho}(\mathbf{r})$  is a weighted density that takes into account the nonlocal structure [24], and

$$\bar{\rho}_{\text{PHE}}(\mathbf{r}) = \int d\mathbf{r}'' \rho(\mathbf{r}'') V_{\text{exc}}^{\text{PHE}}(\mathbf{r} - \mathbf{r}'') \quad (5)$$

is an average density, with  $V_{\text{exc}}^{\text{PHE}}(\mathbf{r})$  being the excluded volume function of two such ellipsoids [see Eq. (12) below]. The choice of a system of parallel ellipsoids as a reference system is particularly convenient because all of its properties can be mapped onto those of a system of hard spheres (whose properties are well documented) with an appropriate scaling along the direction of alignment. Let  $\sigma_{\parallel}$  and  $\sigma_{\perp}$  be the length and breadth of the ellipsoids, respectively. The weighted density is then given by [13]

$$\bar{\rho}(\mathbf{r}) = \int ds w(|\mathbf{s}|; \bar{\rho}(\mathbf{r}) \sigma_{\text{eq}}^3) \rho(\mathbf{r} + \tilde{\sigma} \cdot \mathbf{s}), \quad (6)$$

where  $\sigma_{\text{eq}} \equiv (\sigma_{\perp}^2 \sigma_{\parallel})^{1/3}$  is the equivalent hard-sphere diameter,  $w$  a weight function, and  $\tilde{\sigma}$  a tensor. The integration

variable  $\mathbf{s}$  is dimensionless. The tensor  $\tilde{\sigma}$  is diagonal in the principal-axis frame set by the director  $\hat{\mathbf{n}}$ , with components  $\sigma_{\parallel}$  along the axis parallel to  $\hat{\mathbf{n}}$  and  $\sigma_{\perp}$  along each axis perpendicular to  $\hat{\mathbf{n}}$ . A sensible choice of weight function has been discussed in detail in [24]. Here it suffices to say that  $w$  may be approximated by a quadratic polynomial in  $\bar{\rho}(\mathbf{r})\sigma_{\text{eq}}^3$  which allows us to express the weighted density  $\bar{\rho}(\mathbf{r})$  in terms of three average densities  $\bar{\rho}_n(\mathbf{r})$ ,  $n=0,1,2$ ,

$$\bar{\rho}_n(\mathbf{r}) = \int ds w_n(|\mathbf{s}|) \rho(\mathbf{r} + \tilde{\sigma} \cdot \mathbf{s}). \quad (7)$$

Formulas for  $w_n(s)$  can be found in [24]. We simply note that  $w_0(s) = 3\Theta(1-s)/4\pi$  is a step function and consequently  $\bar{\rho}_0(\mathbf{r})$  is an average over an ellipsoidal volume. Finally, as mentioned before,  $\Psi_{\text{ex}}^{\text{PHE}}(\bar{\rho})$  is the excess free energy per molecule of the fluid of parallel hard ellipsoids, which is equal to that of hard spheres with diameter  $\sigma_{\text{eq}}$ , evaluated at the weighted density  $\bar{\rho}(\mathbf{r})$ . This can be accurately represented by the Carnahan-Starling expression [12].

When the density is uniform, Eq. (4) reduces to the DA, Eq. (2). The ST theory, which can be viewed again as a mapping onto some reference system, in this case a corresponding system of parallel hard ellipsoids, can be applied to different hard-body systems and, in particular, was originally used for hard spherocylinders [5], giving reasonable agreement with simulations (see Sec. IV below).

For a given type of spherocylinder, the question arises as to what are the optimum ellipsoid molecular parameters  $\sigma_{\parallel}$  and  $\sigma_{\perp}$  [which are needed separately in Eq. (6)] to perform the mapping. In contrast with the simpler DA theory, which requires only one condition, here we therefore need two conditions. As a first choice we can start by demanding equal molecular volume  $v$  (hence equal packing fraction) and length-to-breadth ratio for the hard ellipsoids and hard spherocylinders (HSPC's), i.e.,

$$v^{\text{HSPC}} = v^{\text{HE}}, \quad \frac{L+D}{D} = \frac{\sigma_{\parallel}}{\sigma_{\perp}}, \quad (8)$$

where  $L$  and  $D$  are the length of the cylinder and the diameter of the spherical caps, respectively. The condition above of equal length-to-breadth ratio is simpler than the condition originally used by ST, which was based on equal principal values of an averaged inertia tensor. Since  $v^{\text{HSPC}} = \pi D^3 \gamma/6$ , with  $\gamma \equiv 1 + 3\chi/2$  and  $\chi = L/D$ , and  $v^{\text{HE}} = \pi \sigma_{\perp}^2 \sigma_{\parallel}/6 \equiv \pi \sigma_{\text{eq}}^3/6$ , the above equations provide explicit formulas to obtain the relevant dimensions of the effective ellipsoid for a given value of  $\chi = L/D$  of the original spherocylinder:

$$\frac{\sigma_{\parallel}}{\sigma_{\text{eq}}} = (1 + \chi)^{2/3}, \quad \frac{\sigma_{\perp}}{\sigma_{\text{eq}}} = \frac{1}{(1 + \chi)^{1/3}}. \quad (9)$$

For a given value of the average molecular density  $\rho$ , the excess free energy  $\Psi_{\text{ex}}^{\text{PHE}}(\rho)$  is to be evaluated at the packing fraction  $\rho^* \equiv \rho v^{\text{HSPC}} = (\pi/6) \rho \sigma_{\text{eq}}^3$ .

### B. Calculation of the excess free energy

Let us consider a liquid crystal structured along some particular direction; we will choose that direction as the  $z$  axis

and write all densities as a function of  $z$  only. Let us work out the different factors in Eq. (4) and see how they can be simplified. The averaged density  $\bar{\rho}_{\text{PHE}}(\mathbf{r})$  is written as follows:

$$\bar{\rho}_{\text{PHE}}(z) = \int_{-\infty}^{\infty} dz'' \rho(z'') \int d\mathbf{R}'' V_{\text{exc}}^{\text{PHE}}(z-z'', \mathbf{R}-\mathbf{R}'') \quad (10)$$

with  $\mathbf{R} = (x, y)$ . Since

$$V_{\text{exc}}^{\text{PHE}}(z, \mathbf{R}) = \begin{cases} 1, & |z| < \sigma_{\parallel} \sqrt{1 - \frac{x^2 + y^2}{\sigma_{\perp}^2}} \\ 0, & \text{otherwise,} \end{cases} \quad (11)$$

we have

$$\begin{aligned} & \int d\mathbf{R}'' V_{\text{exc}}^{\text{PHE}}(z-z'', \mathbf{R}-\mathbf{R}'') \\ &= \begin{cases} \pi \sigma_{\perp}^2 \left[ 1 - \left( \frac{z-z''}{\sigma_{\parallel}} \right)^2 \right], & 0 \leq |z-z''| \leq \sigma_{\parallel} \\ 0, & |z-z''| > \sigma_{\parallel}, \end{cases} \end{aligned} \quad (12)$$

and it can be readily shown that

$$\bar{\rho}_{\text{PHE}}(z) = \left( \frac{4\pi}{3} \sigma_{\text{eq}}^3 \right) \bar{\rho}_0(z). \quad (13)$$

We now turn to the factor in Eq. (4) containing the double angular integral. This factor can be written in the form

$$\begin{aligned} & \int d\hat{\Omega} \rho(\mathbf{r}, \hat{\Omega}) \int d\mathbf{R}' d\hat{\Omega}' \rho(\mathbf{r}', \hat{\Omega}') V_{\text{exc}}(\mathbf{r}-\mathbf{r}', \hat{\Omega}, \hat{\Omega}') \\ & \equiv \rho(z) \rho(z') \tilde{v}_{\text{SPC}}(z, z'; [f]). \end{aligned} \quad (14)$$

Here  $\tilde{v}_{\text{SPC}}$  is an effective potential that depends on the orientational distribution,

$$\begin{aligned} \tilde{v}_{\text{SPC}}(z, z'; [f]) &= \int d\hat{\Omega} \int d\hat{\Omega}' f(z, \hat{\Omega}) f(z', \hat{\Omega}') \\ & \times \int d\mathbf{R}' V_{\text{exc}}(z-z', \mathbf{R}', \hat{\Omega}, \hat{\Omega}'). \end{aligned} \quad (15)$$

Using ideas proposed in [20] for the Gay-Berne model, we first parametrize the angular distribution function  $f(z, \hat{\Omega})$  in terms of the three order parameters

$$\eta(z) = f_{20}(z) = \int d\hat{\Omega} P_2(\cos \theta) f(z, \hat{\Omega}),$$

$$\sigma(z) = \left( \frac{8}{3} \right)^{1/2} f_{22}(z) = \int d\hat{\Omega} \sin^2 \theta \cos 2\phi f(z, \hat{\Omega}),$$

$$\nu(z) = - \left( \frac{8}{3} \right)^{1/2} f_{21}(z) = \int d\hat{\Omega} \sin 2\theta \cos \phi f(z, \hat{\Omega}), \quad (16)$$

where  $P_2(x)$  is the second-order Legendre polynomial, and  $f_{lm}$  are the coefficients of a general spherical-harmonic expansion for  $f(z, \hat{\Omega})$  in a space-fixed frame. For axially symmetric molecules, this expansion reads

$$f(z, \hat{\Omega}) = \sum_{l=0}^{\infty} \sum_{m=-l}^l \left( \frac{2l+1}{4\pi} \right)^{1/2} f_{lm}(z) Y_{lm}^*(\hat{\Omega}). \quad (17)$$

A biaxial state, such as is expected whenever a tilted director configuration occurs, is characterized by nonvanishing values of  $\sigma$  and  $\nu$ . The actual parametrization that we have used,

$$f(z, \hat{\Omega}) = f(\hat{\Omega}; \eta(z), \sigma(z), \nu(z)), \quad (18)$$

considers only order parameters corresponding to the subspace  $l=2$ , and is written as

$$\begin{aligned} f(\hat{\Omega}; \eta, \sigma, \nu) &= \frac{e^{\Lambda_1 P_2(\cos \theta) + \Lambda_2 \sin 2\theta \cos \phi + \Lambda_3 \sin^2 \theta \cos 2\phi}}{\int d\hat{\Omega} e^{\Lambda_1 P_2(\cos \theta) + \Lambda_2 \sin 2\theta \cos \phi + \Lambda_3 \sin^2 \theta \cos 2\phi}}. \end{aligned} \quad (19)$$

Here  $\{\Lambda_i\}$  are (in principle unknown) functions of  $z$ , which can be thought of as external one-body potentials that set up an orientational structure in the system, characterized by the three order parameters. For each value of  $z$  these potentials can be obtained by inverting Eqs. (16) with  $f(z, \hat{\Omega})$  given by Eq. (19). Thus,  $z$  merely plays the role of an index. Equation (15) for the effective potential  $\tilde{v}_{\text{SPC}}$  then implies

$$\tilde{v}_{\text{SPC}}(z, z'; [f]) = \tilde{v}_{\text{SPC}}(z, z'; [\eta, \sigma, \nu]). \quad (20)$$

Now comes the important approximation in our model, which consists of writing

$$\begin{aligned} \tilde{v}_{\text{SPC}}(z, z'; [\eta, \sigma, \nu]) \approx \tilde{v}_{\text{eff}} \left( z - z'; \frac{\eta(z) + \eta(z')}{2}, \right. \\ \left. \frac{\sigma(z) + \sigma(z')}{2}, \frac{\nu(z) + \nu(z')}{2} \right), \end{aligned} \quad (21)$$

where we define an effective *local* potential as

$$\begin{aligned} \tilde{v}_{\text{eff}}(z; \eta, \sigma, \nu) \equiv \int d\hat{\Omega} \int d\hat{\Omega}' f(\hat{\Omega}; \eta, \sigma, \nu) f(\hat{\Omega}'; \eta, \sigma, \nu) \\ \times \int d\mathbf{R} V_{\text{exc}}(z, \mathbf{R}, \hat{\Omega}, \hat{\Omega}'). \end{aligned} \quad (22)$$

Equations (21) and (22) approximately incorporate nonlocal effects due to spatial inhomogeneities in the order parameters and are exact for a uniform phase. Note that in the limit of a perfectly ordered smectic the approximation also becomes exact since the orientational profile is expected to be independent of  $z$ . Also note that this approximation is exact if one assumes a decoupling between orientations and posi-

tions at the level of the one-particle density. The numerical calculation of  $\tilde{v}_{\text{eff}}$  is explained in Appendix section 1.

Although a spherical-harmonic expansion of the hard-spherocylinder interaction would contain terms with higher angular momentum values  $l$  and therefore the effective potential should be expressed in terms of additional order parameters, it is clear that, within the approximation (19) for the orientational distribution function (which should also include these additional order parameters), the effective potential becomes a functional only of the order parameters  $\eta, \sigma$ , and  $\nu$ .

Our approximation for the excess free-energy functional is then

$$\begin{aligned} F_{\text{ex}}[\rho] = \frac{A}{[(4\pi/3)\sigma_{\text{eq}}^3]} \int_{-\infty}^{\infty} dz \rho(z) \left( \frac{\Psi_{\text{ex}}^{\text{PHE}}(\bar{\rho}(z))}{\bar{\rho}_0(z)} \right) \\ \times \int_{-\infty}^{\infty} dz' \rho(z') \tilde{v}_{\text{eff}} \left( z - z'; \frac{\eta(z) + \eta(z')}{2}, \right. \\ \left. \frac{\mu(z) + \mu(z')}{2}, \frac{\nu(z) + \nu(z')}{2} \right), \end{aligned} \quad (23)$$

where  $A$  is area of the system in the  $xy$  plane. The above description is valid whenever the system of spherocylinders is spatially structured along some direction, which we have taken as the  $z$  direction. In principle, it could be used even if the director is at an angle  $\psi$  with respect to this direction since we have allowed for general values of the order parameters  $\eta, \sigma$ , and  $\nu$ . However, this situation requires modifying (with respect to the untilted case) the calculation of the weighted density by Eq. (6), since the principal-axis frame of the tensor  $\tilde{\sigma}$  is tilted from the space-fixed Cartesian frame by the angle  $\psi$ . It is not difficult to demonstrate (see Appendix section 2) that the averaged density  $\bar{\rho}(z)$  for a system with a tilted director configuration can be written in the same form as in the case of a nontilted configuration but with an effective  $\sigma_{\parallel}$  given by

$$\sigma_{\parallel}^{\text{eff}} = \sigma_{\parallel} \sqrt{\cos^2 \psi + \frac{\sigma_1^2}{\sigma_{\parallel}^2} \sin^2 \psi}, \quad (24)$$

which corrects a relation used in Ref. [19]. The prescription outlined here for the reference hard core is particularly useful in that it is general and can be used in studies of liquid-crystal interfaces in which the interesting phenomenology is associated with inhomogeneities in both density and orientation of the director across the interfaces.

### C. Rotational entropy

Having written the excess term of the free energy in terms of the three  $l=2$  order-parameter components we now turn to the evaluation of the rotational entropy. The ideal free energy of Eq. (1) can be split into translational and rotational parts,

$$\frac{\beta F_{\text{id}}[\rho]}{A} = \int_{-\infty}^{\infty} dz \rho(z) [\ln \Lambda^3 \rho(z) - 1] - \int_{-\infty}^{\infty} dz \rho(z) S_{\text{rot}}(z), \quad (25)$$

where  $\beta=1/kT$  and the local rotational entropy per particle is

$$S_{\text{rot}}(z) = - \int d\hat{\Omega} f(z, \hat{\Omega}) \ln 4\pi f(z, \hat{\Omega}). \quad (26)$$

In [19] it was shown that, if  $f(z, \hat{\Omega})$  is given by Eq. (19), then the rotational entropy can be expressed exactly in terms of the order parameters  $\eta, \sigma, \nu$  as

$$S_{\text{rot}}(z) = \Lambda_1(z) \eta(z) + \Lambda_2(z) \sigma(z) + \Lambda_3(z) \nu(z) - \ln \int \frac{d\hat{\Omega}}{4\pi} \times e^{\Lambda_1(z) P_2(\cos \theta) + \Lambda_2(z) \sin 2\theta \cos \phi + \Lambda_3(z) \sin^2 \theta \cos 2\phi}. \quad (27)$$

To evaluate this entropy for a set of order parameters  $\eta, \sigma, \nu$  we use the scheme explained in the previous section and in Appendix section I to first obtain a table of the numbers  $\Lambda_1, \Lambda_2, \Lambda_3$  as a function of  $\eta, \sigma, \nu$  on a three-dimensional mesh; this table is then interpolated as necessary. Note that this table is calculated once and for all, and that it is also used for the evaluation of the effective potential (see Appendix section I).

### III. ADDITION OF A LINEAR QUADRUPOLE

In this section we augment our model by including a long-range anisotropic term. As mentioned in the Introduction, our aim is to test the capability of the hard-core model as a reference system to describe general nonuniform structures such as smectic-*C* phases. A possible molecular mechanism to produce a tilted director in these phases is a term with quadrupolar symmetry.

We assume each molecule carries a linear quadrupole of magnitude  $\sqrt{|Q|}$ ; the quadrupolar energy associated with two such molecules is taken to be

$$V_Q(\mathbf{r}, \hat{\Omega}, \hat{\Omega}') = Q_V(r) \Gamma(\hat{\mathbf{r}}, \hat{\Omega}, \hat{\Omega}') \quad (28)$$

with

$$\begin{aligned} \Gamma(\hat{\mathbf{r}}, \hat{\Omega}, \hat{\Omega}') &= 1 - 5(\hat{\Omega} \cdot \hat{\mathbf{r}})^2 - 5(\hat{\Omega}' \cdot \hat{\mathbf{r}})^2 \\ &+ 2(\hat{\Omega} \cdot \hat{\Omega}')^2 + 35(\hat{\Omega} \cdot \hat{\mathbf{r}})^2 (\hat{\Omega}' \cdot \hat{\mathbf{r}})^2 \\ &- 20(\hat{\Omega} \cdot \hat{\mathbf{r}})(\hat{\Omega}' \cdot \hat{\mathbf{r}})(\hat{\Omega} \cdot \hat{\Omega}'), \end{aligned} \quad (29)$$

where  $\hat{\mathbf{r}} = \mathbf{r}/r$  and  $r = |\mathbf{r}|$ . The choice of the radial function  $v(r)$  is not critical from the qualitative point of view, since the mechanism giving rise to the molecular tilt comes from the angular symmetry of the interactions. Following our previous studies [19] we take

$$v(r) = \begin{cases} \left[ \left( \frac{\sigma_{\text{eq}}}{r} \right)^{12} - \left( \frac{\sigma_{\text{eq}}}{r} \right)^6 \right], & r > 2^{1/6} \sigma_{\text{eq}} \\ -1/4, & r < 2^{1/6} \sigma_{\text{eq}}. \end{cases} \quad (30)$$

Neglecting anisotropic correlations originating from the hard core, the free energy acquires a mean-field contribution from this anisotropic interaction, which is given by

$$F_Q[\rho] = \frac{1}{2} \int \int d\mathbf{r} d\mathbf{r}' \int \int d\hat{\Omega} d\hat{\Omega}' \rho(\mathbf{r}, \hat{\Omega}) \times \rho(\mathbf{r}', \hat{\Omega}') V_Q(\mathbf{r} - \mathbf{r}', \hat{\Omega}, \hat{\Omega}'). \quad (31)$$

The results of the angular integrals in Eq. (31) can be easily expressed in terms of the order parameters  $\eta, \sigma$ , and  $\nu$  by performing the integral over the relative planar coordinate  $\mathbf{R}' - \mathbf{R}$ :

$$\begin{aligned} \frac{F_Q[\rho]}{A} &= \frac{2Q}{3} \int_{-\infty}^{\infty} dz \rho(z) \int_{-\infty}^{\infty} dz' \rho(z') \tilde{v}(z - z') \\ &\times \left( 6\eta(z)\eta(z') + \frac{3}{4}\sigma(z)\sigma(z') - 3\nu(z)\nu(z') \right), \end{aligned} \quad (32)$$

where

$$\tilde{v}(z) = 2\pi \int_{|z|}^{\infty} dr r v(r) P_4(z/r) \quad (33)$$

and  $P_4(x)$  is the fourth-order Legendre polynomial.

## IV. RESULTS

### A. Hard spherocylinders

We have calculated the coexistence densities for the *N*-*Sm-A*, *N*-*I*, and *I*-*Sm-A* transitions of hard spherocylinders of length-to-breadth ratios  $3.5 \leq L/D \leq 10$ . As usual this was done by computing the free-energy branches corresponding to the different phases involved and applying a Maxwell construction. For a given mean density  $\rho_0$ , the free energy of the *Sm-A* phase was minimized using a four-parameter variational family,

$$\begin{aligned} \rho(z) &= \rho_0 \frac{e^{\lambda \cos(2\pi z/d)}}{\frac{1}{d} \int_0^d dz e^{\lambda \cos(2\pi z/d)}}, \\ \eta(z) &= \eta_0 \frac{e^{\lambda' \cos(2\pi z/d)}}{\frac{1}{d} \int_0^d dz e^{\lambda' \cos(2\pi z/d)}}, \end{aligned} \quad (34)$$

where the variational parameters are  $\lambda, \lambda'$ , which give the amplitude of the spatial modulation in density and order parameter, respectively,  $\eta_0$ , the mean order parameter, and the smectic layer spacing  $d$ . These functions can also describe the nematic phase for which  $\lambda = \lambda' = 0$ . Free-energy minima were obtained using a standard Newton-Raphson minimization algorithm.

Tables I and II contain our results, which are compared with the original calculations by ST [5] of the same model, with theoretical results by Graf and Löwen [10], and with the Monte Carlo simulations of Bolhuis and Frenkel [2]. Our results for the *I*-*N* transition agree closely with those of ST, which in turn are identical to those obtained by Lee [4]; note that the calculations in Refs. [4,5] did not restrict the angular distribution function to the  $l=2$  subspace as was done here

TABLE I. Comparison of the predictions for the coexistence packing fractions  $\rho^* \equiv \rho v^{\text{HSPC}}$  of isotropic ( $\rho_I^*$ ) and nematic ( $\rho_N^*$ ) phases at the  $I$ - $N$  transition, and nematic ( $\rho_N^{*'}$ ) and smectic- $A$  ( $\rho_{\text{Sm}}^*$ ) phases at the  $N$ -Sm $A$  transition from different theories: PW, present work; ST, original Somoza and Tarazona theory [5]; GL, Graf and Löwen theory [10]; MC, results from Monte Carlo simulations of Bolhuis and Frenkel [2]. The asterisk indicates estimates from figures in the source papers.  $n$  indicates that the corresponding phase is not stable; in this case there is a direct  $I$ -Sm- $A$  transition at the indicated coexistence packing fractions.

$L/D$	Theory	$\rho_I^*$	$\rho_N^*$	$\rho_N^{*'}$	$\rho_{\text{Sm}}^*$
3.5	PW	0.483	$n$	$n$	0.525
	ST	0.487	0.499	0.537	0.584
	GL	0.416	$n$	$n$	0.554
	MC	0.491*	$n$	$n$	0.546*
3.8	PW	0.468	0.481	0.485	0.515
	ST	0.466	0.480	0.526	0.580
	GL	0.395*	0.453*	0.453*	0.541*
	MC	0.474	0.474	0.484	0.528
4	PW	0.455	0.469	0.483	0.511
	ST	0.454	0.468	0.513*	0.559*
	GL	0.388*	0.447*	0.454*	0.535*
	MC	0.462*	0.462*	0.479	0.518
4.5	PW	0.426	0.442	0.480	0.506
	ST	0.425	0.441	0.521*	0.568*
	GL	0.367*	0.426*	0.455*	0.529*
	MC	0.432*	0.432*	0.466*	0.500*

in Eq. (19). The present results for the Sm- $A$  phase boundaries differ from those of ST and are significantly closer to the simulations, primarily due to the different criteria used to choose the reference parallel ellipsoids, the relevance of which was recognized by ST. Also, our results are superior to those reported by Graf and Löwen [9] using a modified weighted-density functional theory, which predicts a (wrong) positive slope of the  $N$ -Sm- $A$  phase boundary in the density- $L/D$  phase diagram. In a subsequent paper [10], Graf and Löwen present a hybrid theoretical approach which combines scaled-particle and cell-theory concepts. This theory improves the results for the  $N$ -Sm- $A$  transition in the sense that the slope is now correct, but the predicted density jump is considerably overestimated.

We note that for  $L/D=3.5$ , the Sm- $A$  phase coexists with the isotropic phase while for  $L/D \geq 3.8$ , we find both  $I$ - $N$  and  $N$ -Sm- $A$  transitions. Hence the  $I$ - $N$ -Sm- $A$  triple point is predicted to lie between these values of  $L/D$ , in good agreement with the simulation result  $L/D \approx 3.7$  [2].

Note that our results were obtained *without* the usual decoupling assumption  $f(z, \hat{\Omega}) \equiv f(\hat{\Omega})$  used by ST and other workers (Graf and Löwen [9,10] and Poniewierski and Holyst [6]); however, we find that the coexistence densities change by less than 0.2% for  $L/D=5$  when making this assumption. This insensitivity of the coexistence results to the decoupling assumption is not inconsistent with the statement by van Roij *et al.* [8] concerning the strong spatial

TABLE II. As in Table I but for different values of the length-to-breadth ratio.

$L/D$	Theory	$\rho_I^*$	$\rho_N^*$	$\rho_N^{*'}$	$\rho_{\text{Sm}}^*$
5	PW	0.401	0.418	0.477	0.503
	ST	0.400	0.417	0.507	0.554
	GL	0.339*	0.405*	0.449*	0.530*
	MC	0.398	0.398	0.453	0.482
6	PW	0.358	0.377	0.473	0.496
	ST	0.357	0.377		
	GL			0.443*	0.525*
	MC			0.439*	0.468*
7	PW	0.324	0.344	0.470	0.497
	ST	0.322	0.344		
	GL			0.442*	0.525*
	MC				
10	PW	0.251	0.273	0.465	0.493
	ST	0.251	0.275		
	GL				
	MC	0.245*	0.268*	0.440*	0.450*

modulation of the orientational distribution function in the Sm- $A$  phase of HSPC's: our results show that the variation of  $\eta(z)$  along a smectic period is as high as  $\sim 20\%$ . However, in the neighborhood of the smectic layers, where the number density is highly peaked and the contribution to the free energy is largest, the variation of  $\eta(z)$  over the range where the density is nonzero is significantly smaller than 20% and, as a consequence, the free-energy density is not sensitive to the decoupling assumption.

## B. Hard spherocylinders with quadrupolar interactions

In the Sm- $C$  phase we have to allow for general variations of the three order parameters  $\eta, \sigma, \nu$  to describe tilted director configurations. From a practical point of view it is more convenient to transform to the director (i.e., principal-axis) reference frame by rotating by an angle  $\psi$  (the tilt angle) to obtain  $\eta_p$ , the degree of order around the director, and  $\sigma_p$ , the biaxial order parameter (see Appendix section 1). A simplification can be introduced by assuming that the biaxial order parameter is zero. The relation between the two sets of variables is then

$$\begin{aligned} \eta(z) &= \eta_p(z) P_2(\cos \psi), \\ \sigma(z) &= \eta_p(z) \sin^2 \psi, \\ \nu(z) &= \eta_p(z) \sin 2\psi. \end{aligned} \quad (35)$$

The variational parameters, included in the parametric expressions for  $\rho(z)$  and  $\eta_p(z)$ , are now  $\psi, \eta_{0p}, \lambda, \lambda''$ , and  $d$ , with

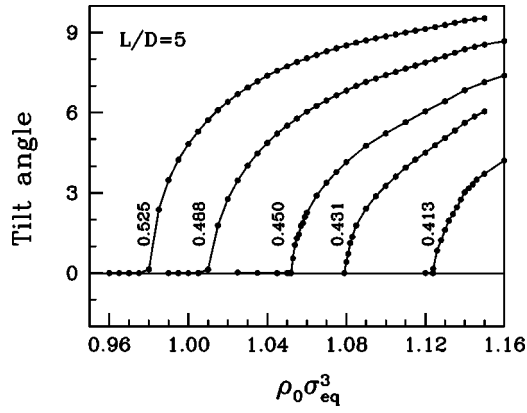


FIG. 1. Tilt angle, in degrees, versus reduced mean density for different values of  $-Q/kT$  and molecular aspect ratio  $L/D=5$ . Continuous lines are a guide to the eye.

$$\eta_p(z) = \eta_{0p} \frac{e^{\lambda'' \cos(2\pi z/d)}}{\frac{1}{d} \int_0^d dz e^{\lambda'' \cos(2\pi z/d)}}. \quad (36)$$

Figure 1 shows the behavior of the tilt angle  $\psi$  with density for different values of the quadrupole strength  $Q/kT$  and for molecules of aspect ratio  $L/D=5$ . Note that, for a given value of the quadrupole strength, the tilt angle eventually adopts a nonzero value as the density is increased, which indicates a transition from a Sm-A to a Sm-C phase. Given that the change in  $\psi$  is continuous in all cases it may be expected that the transition is second order. This is corroborated by examining the free energy and searching for hysteresis loops, which are nonexistent. As is intuitively expected, stronger quadrupoles induce the tilted smectic phase to appear at lower densities. The values of the tilt angle change with density but are of order  $10^\circ$ . This is to be compared with the tilt angles obtained in [19] which were in the range  $35^\circ-40^\circ$ . Our present (lower) values, which are more in accord with experimental findings [25], are due to the better treatment of the hard core. The agreement with experiment is also better concerning the second-order nature of the transition obtained with the present theory, in contrast with the first-order behavior predicted by Velasco *et al.* [19]. On the other hand, we find that the order of the transition changes when considering more elongated molecules. Figure 2 shows

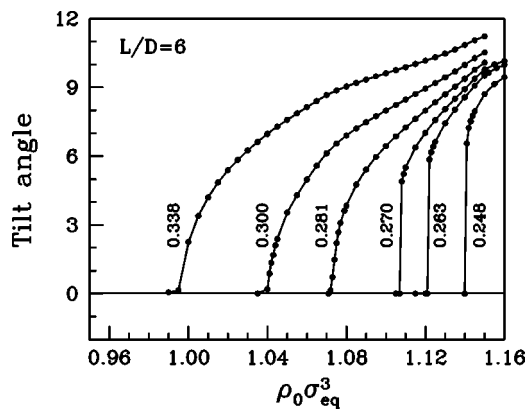


FIG. 2. As in Fig. 1 but for molecular aspect ratio  $L/D=6$ .

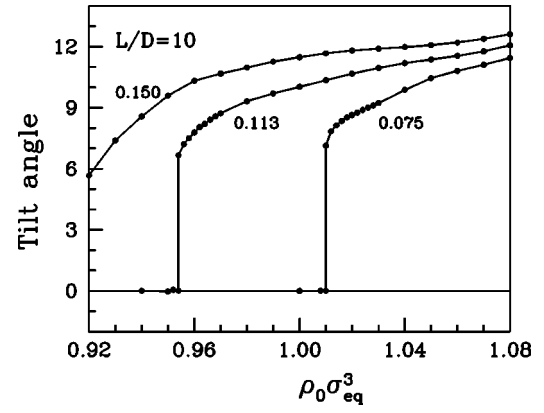


FIG. 3. As in Fig. 1 but for molecular aspect ratio  $L/D=10$ .

that for an aspect ratio  $L/D=6$  the character of the transition changes over from second to first order as the quadrupole strength is decreased. The first-order nature of the transition is signaled by the discontinuous change in tilt angle at some density that depends on the quadrupole strength, and by hysteresis loops present in the free energy. This change in the nature of the transition is associated with the existence of a tricritical point. Note, however, that the tilt-angle jump is less than  $10^\circ$ , so the transition could be considered weakly first order. As the molecular elongation is further increased, the transition becomes first order at lower densities until eventually the whole Sm-A–Sm-C transition line is first order; Fig. 3 shows this for the aspect ratio  $L/D=10$ .

The above results were obtained assuming that the one-molecule distribution function is decoupled, i.e.,  $\lambda''=0$ , since this reduces the computation time considerably. When this approximation is relaxed some quantitative changes occur. This is indicated in Fig. 4 for  $L/D=5$ , which shows that the transition density changes by a few percent, in line with the changes observed in the system of pure hard spherocylinders. However, these changes have no impact whatsoever on the phase behavior from a qualitative point of view.

The complete phase diagram, in the plane  $(\rho_0, Q/kT)$ , is shown in Fig. 5 for elongation  $L/D=5$ . Note that for this case the Sm-A–Sm-C transition is always continuous. Fig-

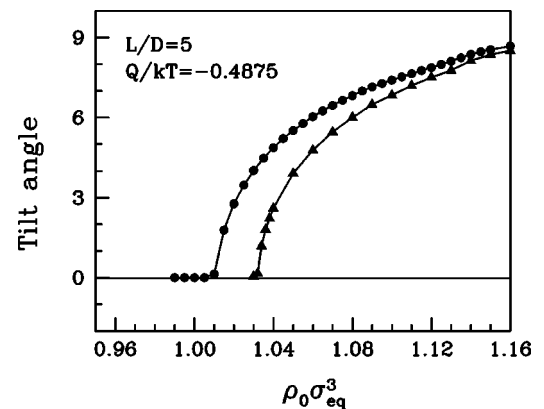


FIG. 4. Tilt angle, in degrees, versus reduced mean density for  $Q/kT=-0.4875$  and molecular aspect ratio  $L/D=5$ . Dots are results obtained with the decoupling assumption, whereas triangles are results obtained without such an assumption. Continuous lines are only a guide to the eye.

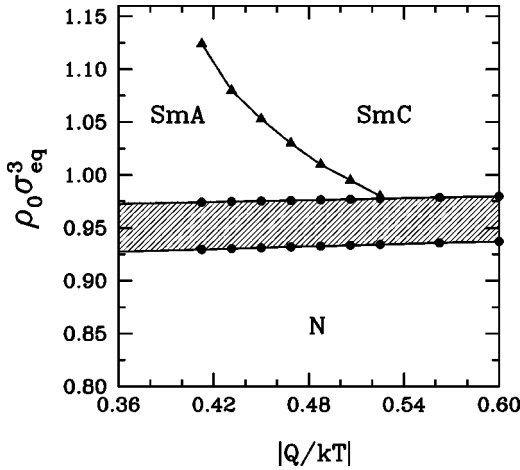


FIG. 5. Phase diagram in the density-quadrupole plane for  $L/D=5$ . Shaded region indicates two-phase coexistence.

ure 5 also shows that the Sm-A phase becomes less stable with increasing quadrupole strength and eventually is preempted by the first-order  $N$ -Sm-C transition.

Finally, Fig. 6 shows the effect of density and quadrupole strength on the equilibrium layer thickness  $d$  for molecular elongation  $L/D=5$ . The data show the existence of two regimes of different average slope, corresponding to the two smectic phases. For a given value of the quadrupole strength, the effect of density on layer thickness in the case of the Sm-A phase is relatively minor, reflecting the low value of the layer compressibility in this system (comparable to that of solids). In the tilted Sm-C phase, however, molecules are tilting and the tilt angle becomes higher as the density increases; therefore the change in layer thickness is more pronounced as it reflects a geometric effect. Likewise, a higher quadrupole strength favors thinner smectic layers as the molecules are more tilted.

## V. CONCLUSIONS

In summary, we have formulated a density-functional theory for inhomogeneous liquid crystals composed of hard spherocylinders having additional long-range interactions of quadrupolar orientational symmetry. Our treatment of the hard-core contribution to the free energy is essentially that

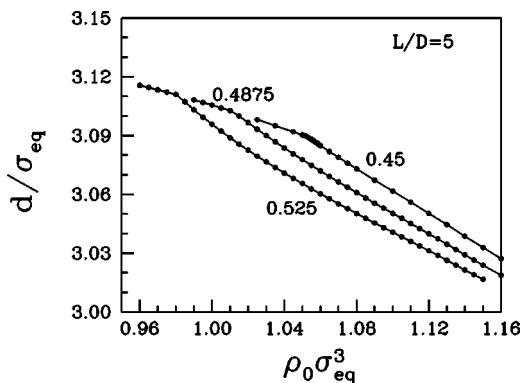


FIG. 6. Smectic layer spacing versus mean density for different values of  $-Q/kT$  and molecular aspect ratio  $L/D=5$ . Continuous lines are only a guide to the eye.

introduced by ST [5] some years ago, but using a simpler prescription for the underlying reference fluid of parallel hard ellipsoids as well as removing the translation-rotation decoupling approximation. The long-range quadrupolar interactions are treated by a simple mean-field approximation. We have also applied several approximations to significantly simplify the numerical calculations. One is the use, which is quite common, of exponential parametrizations of the density and orientational order parameters in modulated phases [see Eqs. (34) and (36)]. The other “numerical” approximations are the truncation of the angular distribution function in the  $l=2$  subspace [Eq. (19)] and use of the “local” approximation [Eqs. (21) and (22)] for the hard-spherocylinder effective potential.

We first applied the theory to calculate the bulk liquid phase boundaries of pure hard spherocylinders. The theory agrees well with simulation data [2] up to elongation  $L/D \approx 5$ , although our results for both the mean density and density gap at the  $N$ -Sm-A transition deteriorate at larger  $L/D$ . The deterioration is much weaker for the  $I$ - $N$  transition, in which case the present theory is in close agreement with the original DA calculations of Lee [4]. This implies that use of the truncated spherical-harmonic representation of the angular distribution function (which is the only difference between our calculations and those of Lee for the uniform nematic phase) does not introduce significant error. While it is difficult to assess whether the discrepancies for the  $N$ -Sm-A transition are due to the other numerical approximations made here or to the basic structure of the density-functional theory itself, the relative accuracy of the former is supported by calculations elsewhere [20]. This suggests that the main limitations are in the underlying density-functional treatment [5] of the inhomogeneous hard-spherocylinder fluid. Nonetheless, the accuracy of the theory for elongations up to  $L/D \approx 5$ , which are realistic for typical thermotropic liquid crystals, is encouraging.

We have not made the translation-rotation decoupling approximation in our calculations, but have demonstrated that this approximation has quite minor effects on bulk phase behavior. This is due to the fact that the spatial modulation of the full distribution function  $\rho(z, \hat{\Omega}) = \rho(z)f(z, \hat{\Omega})$  over a smectic period is due primarily to the number density  $\rho(z)$ . It should be noted that the parametrization employed in Eqs. (19) and (34) for  $f(z, \hat{\Omega})$  is not capable of producing the bimodal behavior observed in computer simulations [8,26]. Since the bimodality occurs only at values of  $z$  between density maxima, its influence on bulk phase behavior should again be very weak.

On including interactions of quadrupolar symmetry, we have shown that the theory can also generate a tilted smectic-C phase. In contrast with the interaction model used in Ref. [19], the present model yields either a continuous or *weakly* first-order Sm-A-Sm-C transition as well as a NAC point. While the Sm-A-Sm-C transition is most often found experimentally to be continuous, first-order transitions have been observed for some optically active compounds and their occurrence is compatible with phenomenological arguments [27]. The present results for SmC behavior are similar to those obtained in Ref. [18], although all transitions in the latter work were found to be continuous. In the present work,



both the  $N$ -Sm-A and  $N$ -Sm-C transitions are first order; hence the NAC point is either a critical end point or a triple point, depending on whether the Sm-A–Sm-C line is continuous or first order, respectively. One drawback that is shared with Ref. [18] is the weak positive slope of the  $N$ -Sm-A and  $N$ -Sm-C coexistence lines in the  $(\rho_0, Q/kT)$  plane, seen in Fig. 5, which produces transitions from Sm-A or Sm-C to nematic on *decreasing* temperature at fixed  $\rho_0$  and  $Q$ . A related drawback is the fact that the Sm-A–Sm-C tricritical point develops on decreasing  $|Q|/kT$ , so that (at fixed  $Q$ ) the transition between those phases changes from continuous to first order with *increasing* temperature. We attribute these features to the particular interaction model used here rather than to approximations in the theory such as its lack of fluctuation effects. True thermotropic liquid crystals should include additional long-range interactions (both isotropic and anisotropic) besides the quadrupolar term considered here (see, e.g., [17,19,20]), which would result in destabilizing the lower-symmetry phases at high temperatures.

We have demonstrated that the theory can feasibly be applied to inhomogeneous liquid crystals with both strongly anisotropic repulsive and attractive interactions. Our work has considered only systems with spatial modulation in one direction, namely, the *liquid* smectic phases. Further study is required to extend the theory to crystalline phases with more than one direction of modulation. The methods described here can be applied directly to the study of liquid interfaces having arbitrary spatial variation of the densities, order parameters, and tilt angle in the  $z$  direction. Most of the numerical techniques described here can be used without modification in such cases, the only exceptions being the parametrizations in Eqs. (34) and (36) of the densities and order parameters.

## APPENDIX

### 1. Calculation of the effective local potential $\tilde{v}_{\text{eff}}$

The effective local potential

$$\begin{aligned} \tilde{v}_{\text{eff}}(z; \eta, \sigma, \nu) = & \int d\hat{\Omega} \int d\hat{\Omega}' f(\hat{\Omega}; \eta, \sigma, \nu) f(\hat{\Omega}'; \eta, \sigma, \nu) \\ & \times \int d\mathbf{R} V_{\text{exc}}(z, \mathbf{R}, \hat{\Omega}, \hat{\Omega}') \end{aligned} \quad (\text{A1})$$

can be numerically computed as follows. Let us first consider the spatial integral

$$\int d\mathbf{R} V_{\text{exc}}(z, \mathbf{R}, \hat{\Omega}, \hat{\Omega}'). \quad (\text{A2})$$

This is numerically equal to the area of a planar section of the excluded volume of two spherocylinders, a complicated volume that depends on the orientations of the spherocylinders, such that their separation in the  $z$  direction is  $z$ . In principle, this area could be computed analytically and integrated numerically over  $\hat{\Omega}, \hat{\Omega}'$  to give the effective potential. We have chosen, however, to represent the whole effective

potential (A1) as a Fourier series [6]. The coefficients of the resulting series are functions of the order parameters  $\eta, \sigma, \nu$  which we have tabulated.

We write

$$\tilde{v}_{\text{eff}}(z; \eta, \sigma, \nu) = \sum_{n=-\infty}^{\infty} v_n(\eta, \sigma, \nu) e^{ik_n z}, \quad k_n = \frac{n\pi}{L+D}, \quad (\text{A3})$$

which is a Fourier representation of the function in the interval  $[-L-D, L+D]$  [note that this is the interval where the function has nonzero values; the periodic replicas outside this interval generated by Eq. (A3) are of no relevance]. The coefficients  $v_n$  are given by

$$\begin{aligned} v_n(\eta, \sigma, \nu) = & \frac{1}{2(L+D)} \int_{-L-D}^{L+D} dz e^{-ik_n z} \\ & \times \left( \int d\hat{\Omega} \int d\hat{\Omega}' f(\hat{\Omega}; \eta, \sigma, \nu) f(\hat{\Omega}'; \eta, \sigma, \nu) \right. \\ & \left. \times \int d\mathbf{R} V_{\text{exc}}(z, \mathbf{R}, \hat{\Omega}, \hat{\Omega}') \right) \\ = & \frac{1}{2(L+D)} \int d\hat{\Omega} \int d\hat{\Omega}' f(\hat{\Omega}; \eta, \sigma, \nu) \\ & \times f(\hat{\Omega}'; \eta, \sigma, \nu) \int_{\text{exc}} d\mathbf{r} e^{-ik_n z}, \end{aligned} \quad (\text{A4})$$

where the integral over  $\mathbf{r}$  now extends over the excluded volume. This integral is much easier to calculate than that in Eq. (A2). In order to exploit the symmetries of the excluded volume, it is convenient to perform a rotation of axes to a frame with axes along the principal axes  $\{\hat{\mathbf{u}}_i\}$  of the excluded volume,

$$\hat{\mathbf{u}}_1 = \frac{\hat{\Omega} \times \hat{\Omega}'}{|\hat{\Omega} \times \hat{\Omega}'|}, \quad \hat{\mathbf{u}}_2 = \frac{\hat{\Omega} + \hat{\Omega}'}{|\hat{\Omega} + \hat{\Omega}'|}, \quad \hat{\mathbf{u}}_3 = \frac{\hat{\Omega} - \hat{\Omega}'}{|\hat{\Omega} - \hat{\Omega}'|}. \quad (\text{A5})$$

Since the Jacobian of this transformation is unity, it follows that

$$\int_{\text{exc}} d\mathbf{r} e^{-ik_n z} = \int_{\text{exc}} d\mathbf{u} e^{-ik_n \cdot \mathbf{u}}, \quad (\text{A6})$$

where  $\mathbf{k}_n$  is a vector of magnitude  $k_n$  in the space-fixed  $z$  direction. The limits of integration are easily written in this frame and the integrals can be evaluated by Gaussian quadrature. The wave vector  $\mathbf{k}_n$  becomes angle dependent when expressed in the principal-axis frame.

The coefficients  $v_n(\eta, \sigma, \nu)$  can now be evaluated for different values of the order parameters and a table with three entries can be constructed. Values of the coefficients for order parameters not in the table are obtained by interpolation. We have found that it is numerically more convenient to construct the table with  $\eta_p, \sigma_p, \psi$  as entries, where  $\psi$  is the tilt angle and  $(\eta_p, \sigma_p)$  the uniaxial and biaxial order parameters in the principal-axis frame, respectively. Transformation from one set to the other is obtained via the expressions

$$\begin{aligned}\eta &= \eta_p P_2(\cos \psi) + \frac{3}{4} \sigma_p \sin^2 \psi, \\ \sigma &= \eta_p \sin^2 \psi + \frac{1}{2} \sigma_p (1 + \cos^2 \psi), \\ \nu &= \eta_p \sin 2\psi - \frac{1}{2} \sigma_p \sin 2\psi.\end{aligned}\quad (\text{A7})$$

Another question is the number of Fourier components used to represent the function. Clearly  $\tilde{v}_{\text{eff}}(z; \eta, \sigma, \nu)$  is an even function of  $z$ , which means that only coefficients with  $n \geq 0$  are necessary. We have found that a reasonable accuracy is obtained using only 21 Fourier components.

## 2. Scaling of the system of parallel ellipsoids for the smectic-C phase

Let us consider the weighted densities in Eq. (7),

$$\bar{\rho}_n(\mathbf{r}) = \int ds w_n(s) \rho(\mathbf{r} + \tilde{\sigma} \cdot \mathbf{s}). \quad (\text{A8})$$

In the space-fixed system of Cartesian axes, we assume that the density  $\rho(\mathbf{r})$  varies only in the  $z$  direction. In the smectic-C phase, the molecules are tilted by an angle  $\psi$  with respect to the  $z$  axis. However, the tensor  $\tilde{\sigma}$  is diagonal only in an axis frame along the principal molecular axes, which are now rotated with respect to the space-fixed axes by the angle  $\psi$ .

The argument of the density in the integrand of Eq. (A8) is  $\mathbf{r} + \tilde{\sigma} \cdot \mathbf{s} \equiv \mathbf{r} + \mathbf{r}'$  with  $\mathbf{r}' = \tilde{\sigma} \cdot \mathbf{s}$ . In the principal-axis frame of the tilted molecules  $\tilde{\sigma}$  is diagonal. Let us denote the components of  $\mathbf{r}'$  and  $\mathbf{s}$  in this frame by subscripts and superscripts  $p$ , respectively, so that

$$\begin{pmatrix} x'_p \\ y'_p \\ z'_p \end{pmatrix} = \begin{pmatrix} \sigma_{\perp} s_x^p \\ \sigma_{\perp} s_y^p \\ \sigma_{\parallel} s_z^p \end{pmatrix}. \quad (\text{A9})$$

Now we calculate the corresponding components of  $\mathbf{r}'$  in the original space-fixed axis frame. We assume that the director lies in the  $xz$  plane. By rotating about the  $y$  axis by  $\psi$ , we obtain

$$\begin{aligned}x' &= x'_p \cos \psi + z'_p \sin \psi, \\ y' &= y'_p, \\ z' &= -x'_p \sin \psi + z'_p \cos \psi.\end{aligned}\quad (\text{A10})$$

Substituting for  $x'_p$  and  $z'_p$  from Eq. (A9),

$$z' = -\sigma_{\perp} s_x^p \sin \psi + \sigma_{\parallel} s_z^p \cos \psi. \quad (\text{A11})$$

Now the density  $\rho(\mathbf{r} + \mathbf{r}')$  in Eq. (A8) varies only in the  $z$  direction, so we can write

$$\rho(\mathbf{r} + \mathbf{r}') = \rho(z + z'), \quad (\text{A12})$$

where  $z'$  is given by Eq. (A11). We can do a further transformation of the vector  $\mathbf{s}$  in Eq. (A8). Let us rotate from the principal-axis frame back to a new frame, by an arbitrary (for now) angle  $\psi_p$ . Let us call the components of  $\mathbf{s}$  in this new frame simply  $(s_x, s_y, s_z)$ . These will be related to the components  $(s_x^p, s_y^p, s_z^p)$  by the analogs of Eq. (A10). The inverse relations are

$$\begin{aligned}s_x^p &= s_x \cos \psi_p - s_z \sin \psi_p, \\ s_y^p &= s_y, \\ s_z^p &= s_x \sin \psi_p + s_z \cos \psi_p.\end{aligned}\quad (\text{A13})$$

Note that this is an orthogonal transformation and consequently the magnitude of  $\mathbf{s}$  is preserved, so that  $w_n(|\mathbf{s}|)$  is the same function in both frames, and the Jacobian of the transformation is unity. On substituting Eq. (A13) into Eq. (A11), we obtain

$$\begin{aligned}z' &= s_x (\sigma_{\parallel} \cos \psi \sin \psi_p - \sigma_{\perp} \sin \psi \cos \psi_p) \\ &\quad + s_z (\sigma_{\parallel} \cos \psi \cos \psi_p + \sigma_{\perp} \sin \psi \sin \psi_p).\end{aligned}\quad (\text{A14})$$

As mentioned,  $\psi_p$  is arbitrary. It would be convenient if we could choose  $\psi_p$  so that the coefficient of  $s_x$  in Eq. (A14) is zero. This gives the equation

$$\sigma_{\parallel} \cos \psi \sin \psi_p = \sigma_{\perp} \sin \psi \cos \psi_p \quad (\text{A15})$$

or

$$\tan \psi_p = \frac{\sigma_{\perp}}{\sigma_{\parallel}} \tan \psi. \quad (\text{A16})$$

Remember that  $\psi$  is the smectic-C tilt angle, which physically satisfies  $0 \leq \psi \leq \pi/2$ . Since (normally)  $\sigma_{\perp} / \sigma_{\parallel} < 1$ , we can always find a unique solution of Eq. (A16) with  $0 \leq \psi_p \leq \pi/2$ . Now Eq. (A14) simplifies to

$$\begin{aligned}z' &= s_z (\sigma_{\parallel} \cos \psi \cos \psi_p + \sigma_{\perp} \sin \psi \sin \psi_p) \\ &= s_z \sigma_{\parallel} \cos \psi \cos \psi_p \left( 1 + \frac{\sigma_{\perp}}{\sigma_{\parallel}} \tan \psi \tan \psi_p \right).\end{aligned}\quad (\text{A17})$$

Using Eq. (A16) and trigonometric relations, this becomes

$$z' = s_z \sigma_{\parallel} \sqrt{\cos^2 \psi + \frac{\sigma_{\perp}^2}{\sigma_{\parallel}^2} \sin^2 \psi} \equiv s_z \sigma_{\parallel}^{\text{eff}}. \quad (\text{A18})$$

The identity in Eq. (A12), which is in the integrand of Eq. (A8), becomes

$$\rho(\mathbf{r} + \mathbf{r}') = \rho(z + s_z \sigma_{\parallel}^{\text{eff}}). \quad (\text{A19})$$

This is analogous to the case of the smectic-A phase, but with an *effective*  $\sigma_{\parallel}$  given by Eq. (24) in the text. Notice that  $\sigma_{\parallel}^{\text{eff}} = \sigma_{\parallel}$  when  $\psi = 0$  while  $\sigma_{\parallel}^{\text{eff}} = \sigma_{\perp}$  when  $\psi = \pi/2$ .

- [1] L. Onsager, Ann. (N.Y.) Acad. Sci. **51**, 627 (1949).
- [2] P. Bolhuis and D. Frenkel, J. Chem. Phys. **106**, 666 (1997).
- [3] S. C. McGrother, D. C. Williamson, and G. Jackson, J. Chem. Phys. **104**, 6755 (1996).
- [4] S.-D. Lee, J. Chem. Phys. **87**, 4972 (1987).
- [5] A. M. Somoza and P. Tarazona, Phys. Rev. Lett. **61**, 2566 (1988); Phys. Rev. A **41**, 965 (1990).
- [6] A. Poniewierski and R. Holyst, Phys. Rev. Lett. **61**, 2461 (1988).
- [7] B. Tjpto-Margo and G. Evans, Mol. Phys. **74**, 85 (1991).
- [8] R. van Roij, P. Bolhuis, M. Mulder and D. Frenkel, Phys. Rev. E **52**, R1277 (1995).
- [9] H. Graf and H. Löwen, J. Phys.: Condens. Matter **11**, 1435 (1999).
- [10] H. Graf and H. Löwen, Phys. Rev. E **59**, 1932 (1999).
- [11] B. Jérôme, Rep. Prog. Phys. **54**, 391 (1991).
- [12] J. P. Hansen and I. R. McDonald, *Theory of Simple Liquids* (Dekker, New York, 1986).
- [13] L. Mederos and D. E. Sullivan, Phys. Rev. A **39**, 854 (1989).
- [14] R. G. Priest, J. Phys. (Paris) **36**, 437 (1975).
- [15] P. G. de Gennes and J. Prost, *The Physics of Liquid Crystals* (Clarendon, Oxford, 1993).
- [16] E. Martn del Rio, M. M. Telo da Gama, E. de Miguel, and L. F. Rull, Phys. Rev. E **52**, 5028 (1995).
- [17] F. N. Braun, T. J. Sluckin, E. Velasco, and L. Mederos, Phys. Rev. E **53**, 706 (1996).
- [18] A. Poniewierski and T. J. Sluckin, Mol. Phys. **73**, 199 (1991).
- [19] E. Velasco, L. Mederos, and T. J. Sluckin, Liq. Cryst. **20**, 399 (1996).
- [20] E. Velasco and L. Mederos, J. Chem. Phys. **109**, 2361 (1998).
- [21] J. D. Parsons, J. Chem. Phys. **19**, 1225 (1979).
- [22] It is common in the literature to use the term *decoupling approximation* in the context used here, i.e., to refer to a decoupling between translational and orientational degrees of freedom at the level of the excluded volume and *not* at the level of the one-particle density.
- [23] A. M. Somoza and P. Tarazona, J. Chem. Phys. **91**, 517 (1989).
- [24] P. Tarazona, Phys. Rev. A **31**, 2672 (1985).
- [25] J. Doucet, A. M. Levelut, and M. Lambert, Mol. Cryst. Liq. Cryst. **24**, 317 (1973).
- [26] J. S. van Duijneveldt and M. P. Allen, Mol. Phys. **90**, 243 (1997).
- [27] T. Stoebe, L. Reed, M. Veum, and C. C. Huang, Phys. Rev. E **54**, 1584 (1996).